Bruce A. Finlayson

ICCAD

INTERNATIONAL CENTRE FOR
COMPUTER AIDED DESIGN

SECOND
INTERNATIONAL SYMPOSIUM ON

FINITE ELEMENT METHODS IN FLOW PROBLEMS

S. MARGHERITA LIGURE (ITALY)-JUNE 14-18, 1976

PREPRINTS

CONFERENCE SERIES N° 2/76

ICCAD

International Centre for Computer Aided Design

second
INTERNATIONAL SYMPOSIUM
on
FINITE ELEMENT METHODS
in
FLOW PROBLEMS

Santa Margherita Ligure (Italy) June 14 - June 18, 1976

COLLOCATION FINITE ELEMENT CALCULATIONS FOR FLUID FLOW, HEAT AND MASS TRANSFER IN MONOLITH CHEMICAL REACTORS

L.C. Young, B.A. Finlayson
(U.S.A.)

SESSION 7: REACTING FLOW, DIFFUSION AND CONVECTION

COLLOCATION FINITE ELEMENT CALCULATIONS FOR FLUID FLOW, HEAT AND MASS TRANSFER IN MONOLITH CHEMICAL REACTORS

Larry C. Young
Amoco Production Res.
Tulsa, Okla., USA

Bruce A. Finlayson
Dept. Chemical Engineering
University of Washington
Seattle, Wash. 98195, USA

1. Summary

A collocation method combines global polynomial expansions and polynomial expansions on finite elements to solve for the fluid flow, heat and mass transfer in monolith chemical reactors. The monolith is modeled as a tube for fluid flow with reaction on the walls. The equations governing heat and mass transfer in the fluid and solid wall are solved in three dimensions, including steady state and transient simulations, for conditions typical of the treatment of automobile exhaust gases to oxidize carbon monoxide.

2. Equations

A monolith chemical reactor consists of about a thousand small tubes, whose walls are formed by a ceramic material. Figure 1a illustrates schematically part of the end view of such devices. The solid walls are coated with porous alumina, on which is deposited a catalyst. Platinum is widely used in the United States, when such reactors are placed in the exhaust stream of an automobile. Any carbon monoxide in the engine exhaust is reacted with oxygen to produce harmless carbon dioxide before the exhaust gases are emitted to the atmosphere.

These reactors are modeled here by assuming that each cell can be modeled independently, that is the cell is adiabatic and good flow distribution insures equal flow rates in all cells. Justification and limitations on these and other assumptions are given elsewhere (Young and Finlayson, 1976).

2.1 Fluid Flow

The fluid flow in each tube is laminar, since even at highway cruising speeds the maximum Reynolds number is 600. The region of developing velocity profiles is neglected; fully developed flow is assumed governed by the equation:

$$\mu\left(\frac{\partial^2 u}{\partial x^2} + \frac{\partial^2 u}{\partial y^2}\right) = \frac{dP}{dz} \text{ in } A \qquad (1)$$

$$u(x,y) = 0 \qquad \text{on } C \qquad (2)$$

Here μ is the axial velocity in the z-direction, x and y are transverse directions, μ is viscosity, dP/dz is the pressure gradient, A is the open region of the ducts illustrated in Figure 2, while C is the boundary between the open region and solid wall. The relation of the axial direction z and the transverse directions x and y is apparent by compa-

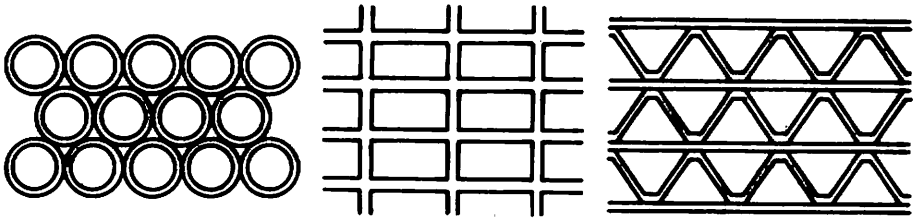

Fig. 1a. End View of Typical Monolith Geometries

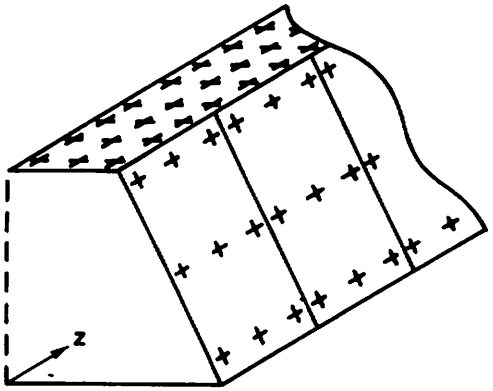

Fig. 1b. Location of Collocation Points on Solid in Axial Direction

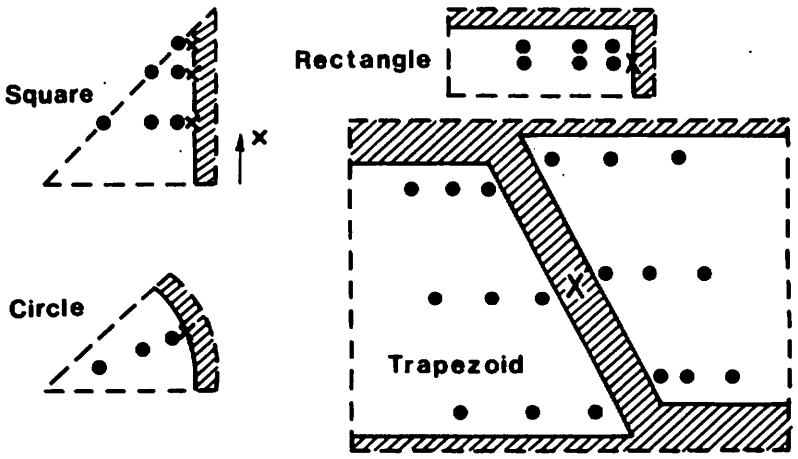

Fig. 2. Symmetric Portions of Monolith Geometries
Fluid, Solid Collocation Points

rison of Figure 1b and 2. We take the viscosity constant.

2.2 Heat and Mass Transfer in the Fluid

The energy and mass balances in the fluid are

$$C_p u(x,y) \frac{\partial T^f}{\partial z} = k^f \left(\frac{\partial^2}{\partial x^2} + \frac{\partial^2}{\partial y^2}\right) T^f \tag{3}$$

$$u(x,y) \frac{\partial Y^f}{\partial z} = D^f \left(\frac{\partial^2}{\partial x^2} + \frac{\partial^2}{\partial y^2}\right) Y^f \tag{4}$$

where T^f is the fluid temperature, Y^f is the mole fraction of a species (here carbon monoxide), C_p is the mass heat capacity, k^f is the fluid thermal conductivity and D^f is the diffusivity of carbon monoxide in the gas. This can be taken as an effective multicomponent diffusivity. We also assume the gas is ideal, the total concentration is constant, and the carbon monoxide is dilute. In both Eqs. (3-4) we have allowed transverse conduction and diffusion in the x- and y-directions, but have neglected it in the z-direction compared to convection. The transient terms have been neglected in Eqs. (1,3,4) because the fluid responds thousands of times faster than the solid temperature, leading to the quasi-static approximation (see Young and Finlayson, 1976).

2.3 Heat and Mass Transfer in the Solid

The solid walls illustrated in Figure 2 are all relatively thin, and we approximate them by assuming there are no temperature variations across the thickness. There may be temperature variations around the periphery, as in Figure 2, or along the length, as in Figure 1b. The reaction layer of catalyst on porous alumina is even thinner, and we model it as a surface reaction, although in the equations below the thickness is ζ. The thermal conductivities of the porous alumina and the ceramic substract (walls) are taken as the same, and diffusion can occur in the porous layer, but not the ceramic substrate. The equations are then

$$\rho^s C_p{}^s \frac{\partial T^s}{\partial t} - k^s \frac{\partial^2 T^s}{\partial z^2} - \frac{k^s}{(2r_h+d/4)^2} \frac{\partial^2 T^s}{\partial x^2} + \frac{k^f}{r_{hs}} \underset{\sim}{n}\cdot\nabla T^f + \frac{(-\Delta H_R)\zeta\, r}{r_{hs}} = 0 \tag{5}$$

$$\varepsilon_s \zeta \frac{\partial Y^s}{\partial t} - \zeta D^s \frac{\partial^2 Y^s}{\partial z^2} - \frac{\zeta\, D^s}{(2r_h)^2} \frac{\partial^2 Y^s}{\partial x^2} + D^f \underset{\sim}{n}\cdot\nabla Y^f + \frac{\zeta r}{C} = 0 \tag{6}$$

where $\rho^s C_p{}^s$ is the solid heat capacity per unit volume, T^s is the solid temperature and is a function of x, z and t, k^s is the solid thermal conductivity, d is the wall thickness, r_{hs} is the hydraulic radius of the solid, the solid cross sectional area shown in Figure 2 divided by the perimeter of contact between the solid and fluid. The rate of reaction is r in units of mole per time per volume, the heat of reac-

tion is $-\Delta H_R$, ϵ_s is the void fraction of the porous alumina, Y^s is the concentration of gas in the pores of the alumina. D^s is the effective diffusivity in the solid and t is the time. The third term in Eqs. (5-6) involves $\partial^2/\partial x^2$. This term represents conduction and diffusion in the wall of the square duct, Figure 2, and is normalized to go from 0 to 1 for the limits shown in Figure 2. This term is kept in the equations only for the square geometry. In the other geometries it is assumed that peripheral conduction and diffusion is infinitely fast and no temperature or concentration variations can occur around the periphery in the solid. Then it is necessary to have only one collocation point in the solid, as illustrated in Figure 2. This assumption is tested in the calculations reported below.

2.4 Reaction Rate Expression

The rate of reaction of carbon monoxide and oxygen on platinum shows that the rate of reaction is inversely proportional to carbon monoxide concentration. Here we use a rate expression which is essentially that measured by Harned (1972).

$$-r = k_1 Y^s_{O_2} Y^s_{CO} / [Y^s_{O_2} + k_2 (Y^s_{CO})^2] \qquad (7)$$

For CO concentrations above 1% the second term in the denominators predominates, giving $r \alpha (Y^s_{CO})^{-1}$. Oxygen is in excess, so that $Y^s_{O_2} \approx$ constant, and the first term in the denominator is important only at very low CO concentrations. The heat effects of the reaction of hydrogen is included in $-\Delta H_R$ (see Young and Finlayson, 1976).

2.5 Boundary Conditions

On the surface between the fluid and solid the fluid temperature equals the solid temperature. For the dotted lines in Figure 2 a symmetry condition is applied. In the fluid this is done automatically by the orthogonal collocation method. Boundary conditions are written at the inlet to the monolith by regarding the region outside the monolith as a well-stirred vessel with uniform temperature. At the exit we take the usual condition that variations in the z-direction are zero. Initial conditions must also be specified for all variables.

3. Solution Method

The model requires finding the solution for $u(x,y)$, T^f and Y^f as functions of x, y, and z, and T^s and Y^s as functions of x, z, and t (for the square) or z and t (for the other duct shapes).

3.1 Velocity

Global orthogonal collocation (Finlayson, 1972) is used to solve Eq. (1). The high convergence properties of global orthogonal polynomials insures that only a few terms are necessary in the expansion. The irregular geometries in Figure 2 are transformed to a regular geometry (square, rectangle, or circle) before orthogonal collocation is applied. For the square we get

$$\sum_{k=1}^{N} B^x_{ik}\, u_{kj} + \sum_{k=1}^{M} B^y_{jk}\, u_{ik} = \frac{b^2}{\mu}\frac{dP}{dz} \qquad (8)$$

$$i=1,\ldots,N;\quad j=1,\ldots,M$$

where 2b is the length of the side of square, B^x_{ik} and B^y_{jk} are collocation matrices derived elsewhere (Finlayson, 1972, 1974) and $u_{kj} = u(x_k,y_j)$ is the velocity at the collocation point (x_k,y_j). On the boundary $u_{kj}=0$. Equation (8), which represents the residual at the collocation point, is thus satisfied at the NM interior collocation points denoted by • in Figure 2.

3.2 Fluid Temperature and Concentration

Eqs. (3-4) are solved using global orthogonal collocation in the x,y-directions and continuously using an eigenfunction expansion in the z-direction. The solution method is illustrated for temperature in a circular geometry. For an arbitrary wall temperature distribution $T_w(z)$, the exact solution for $T^f(x,z)$ is

$$T^f(x,z) = T_c - \sum_{n=1}^{\infty} \lambda_n C_n R_n(x) \int_0^z e^{\lambda_n(z-\tau)} [T_w(\tau)-T_o]d\tau \qquad (9)$$

where λ_n are the eigenvalues and $R_n(x)$ the eigenfunctions for the Graetz problem with $T_w(z)$ = constant. The orthogonal collocation approximation to this, evaluated at the collocation points x_i, is

$$T^f(x_i,z) = T_o + \sum_{j=1}^{N}\sum_{n=1}^{N} V_{in} V^{-1}_{nj} (1-x_j^2) B_{j,N+1} \times \int_0^z e^{\lambda_n(z-\tau)} [T_w(\tau)-T_o]d\tau \qquad (10)$$

where now λ_n and V_{in} represent the eigenvalues of the approximate solution and the eigenvectors of the eigenvalue problem. The fluid temperature and concentration in other geometries is derived in a similar way; even though an exact solution (9) may not be possible in the irregular geometries, the orthogonal approximation (10) is possible provided the shape of the duct is one that is transformable to a regular domain. Eqs. (9) represents, essentially, a Green's function for Eqs. (3), and Eqs. (10), even in other geometries, is an approximation to the Green's function. The global orthogonal collocation method, with the expansion functions orthogonal polynomials defined over the whole domain, are used here, too, because only a few terms are needed to insure highly accurate results.

3.3 Solid Temperature and Concentration

After solving for the fluid temperature as in Eqs. (10), and for fluid concentration in a like manner, the terms $\underset{\sim}{n}\cdot\nabla T^f$ and $\underset{\sim}{n}\cdot\nabla Y^f$ are calculated for insertion in Eqs. (5-6). The result is an integro-differential equation for $T^s(z,x,t)$ and $Y^s(z,x,t)$. The advantage of this solution method is that all the collocation points in the fluid are eliminated as unknowns; this reduces the number of unknowns by a factor between 3 and 15, depending on the situation. We still have a partial

differential equation to solve. Global orthogonal collocation is applied in the x-direction, since the profiles are expected to be smooth. Orthogonal collocation on finite elements (Carey and Finlayson, 1975) is applied in the z-direction since the profiles are steep in that direction, which would require a large number of terms in a global expansion. Usually 10-25 elements were used in the z-direction and a 6th degree polynomial was employed on each element. The equations are assembled and solved iteratively, element by element, from the inlet to the outlet, and then repeating the sweep as often as is necessary.

4. Results

The simulation results for a PTX-4 Englehard converter are given in Figures 3-8. They are especially interesting in that multiple steady-state solutions are possible for the same inlet and boundary conditions.

4.1 Multiple Steady-States

Temperature and concentration profiles are shown down the reactor in Figure 3 for conditions of $T_o^f = 587^oF$, $Y_o^f = 0.04$, Re = 160. We see that the solid temperature rises sharply (light off) and the fluid temperature increases more gradually. The concentration profiles are almost a mirror image of the temperature profiles. One of the steady-state solutions, however, does not light off and very little reaction takes place. Which of these solutions occurs depends on the past history of the reactor.

The hysteresis effect is illustrated in Figure 4. Such curves have been obtained experimentally by Hlaváček and Votruba (1974) in the following manner. Beginning with a cold reactor, desired inlet conditions are maintained at a low temperature until steady-state has been reached, giving one data point on the top part of the curve. Then the inlet temperature is raised, and the experiment again proceeds to steady-state, giving another data point. This procedure is followed giving the curve denoted by →. At the ignition temperature light off occurs and the concentration of carbon monoxide out of the reactor decreases drastically. Almost complete conversion is obtained for any higher inlet temperature. Then the inlet temperature is lowered, step by step, giving rise to the curve marked ←. At the extinction temperature the concentration suddenly increases and little reaction takes place. The two profiles shown in Figure 3 then represent two cases - one with light off, the other nearly extinguished.

The slight effect of geometry of the duct on the hysteresis curves is indicated in Table I by listing the extinction and ignition temperature.

Table I
Extinction and Light Off Temperatures for Different Geometries

Geometry	$T_{extinction}(^oF)$	$T_{ignition}(^oF)$
square	575	575-587
circle	587-591	587-591
trapezoid	587-591	591-595
rectangle	595-600	595-600

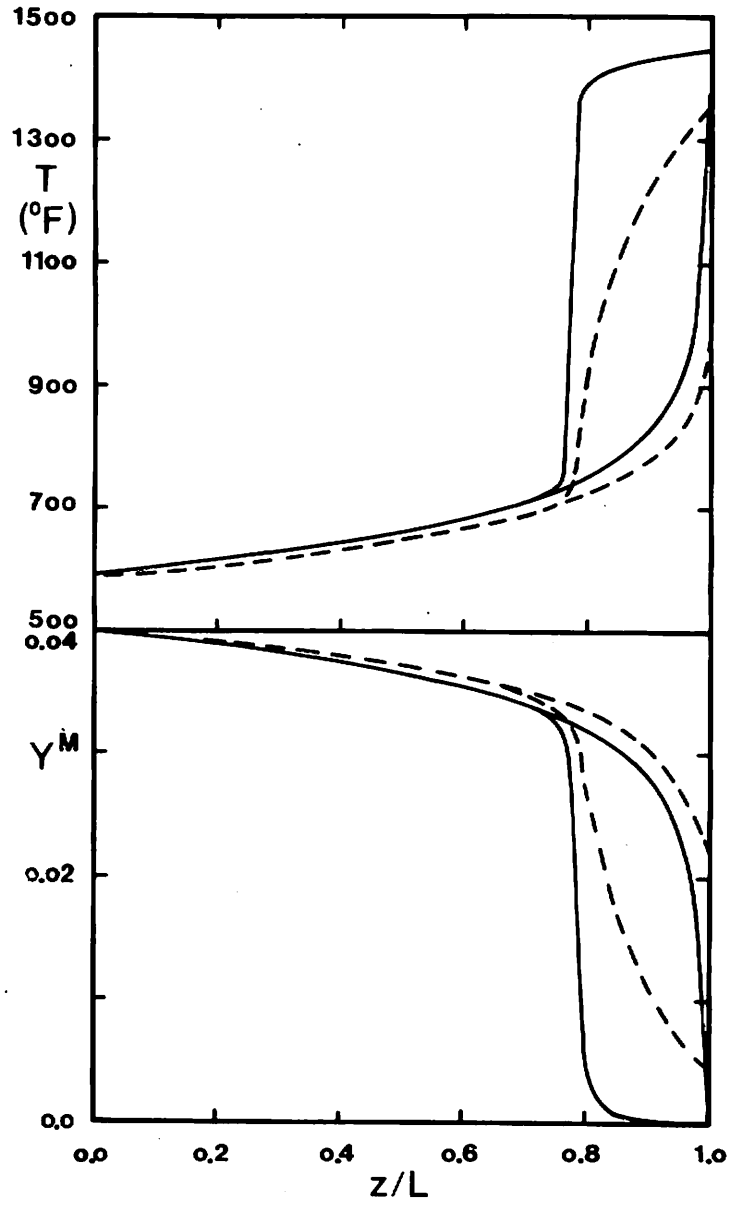

Fig. 3. Temperature and Concentration Profiles Down Reactor
——— Solid, – – – Fluid

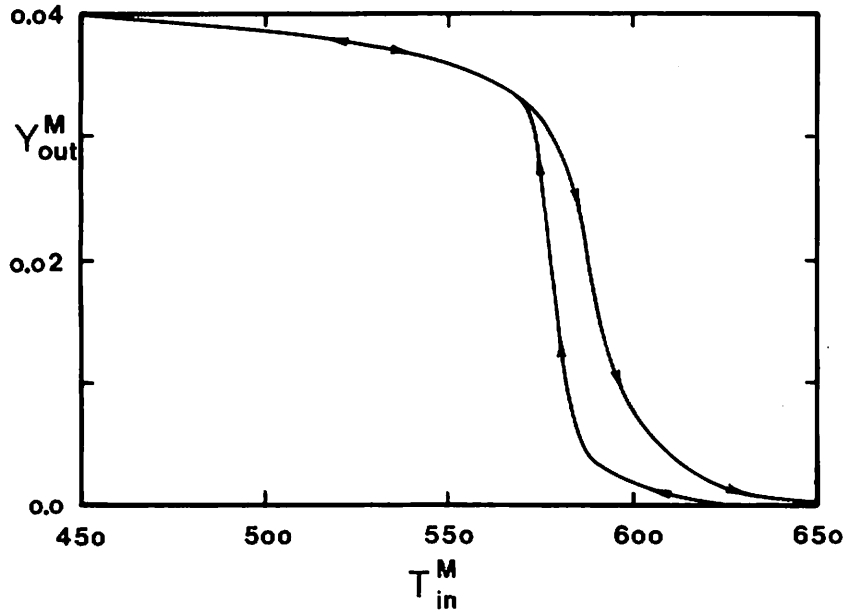

Fig. 4. Hysteresis Curve

4.2 Transient Simulations

Figure 5 shows how the solid temperature changes when the gas flow rate suddenly increases. Initially the solid temperature is at 1087°F and the fluid mole fraction in the porous solid is Y^S=0. At time zero a flow is established with T^f_o = 700°F, Y^f_o = 0.02, and a flow rate of 80 std.ft.^{3}/min. (Re = 449). The reactor is cooling, and as it does so the front (where light off occurs) moves downstream slowly. If the temperature were decreased more, or the flow rate increased more, the front would move downstream and could move out the end of the reactor, which is called blow out.

4.3 Effect of Different Models

Figure 6 shows the mole fraction profiles for three different models to test the importance of certain terms in Eqs. (5). Curve 1 corresponds to setting k_s=0 in the axial conduction term, which allows no axial conduction of heat, and k_s=∞ in the peripheral (x)-direction, which uses very fast conduction around the periphery. This last case can be solved using only a single collocation point in the x-direction, as shown in Figure 2. Curve 2 of Figure 6 permits axial conduction of heat, but still uses only a single collocation point in the x-direction, while curve 3 is for the complete model governed by Eqs. (5). We see that in this case neither the effect of axial heat conduction or finite peripheral heat conduction has a large bearing on the results. Other simulations (Young and Finlayson, 1976) indicate that models having axial conduction can have multiple steady-states (giving rise to hysteresis) whereas models without axial conduction are unique (no hysteresis). Thus axial conduction must be included. The peripheral

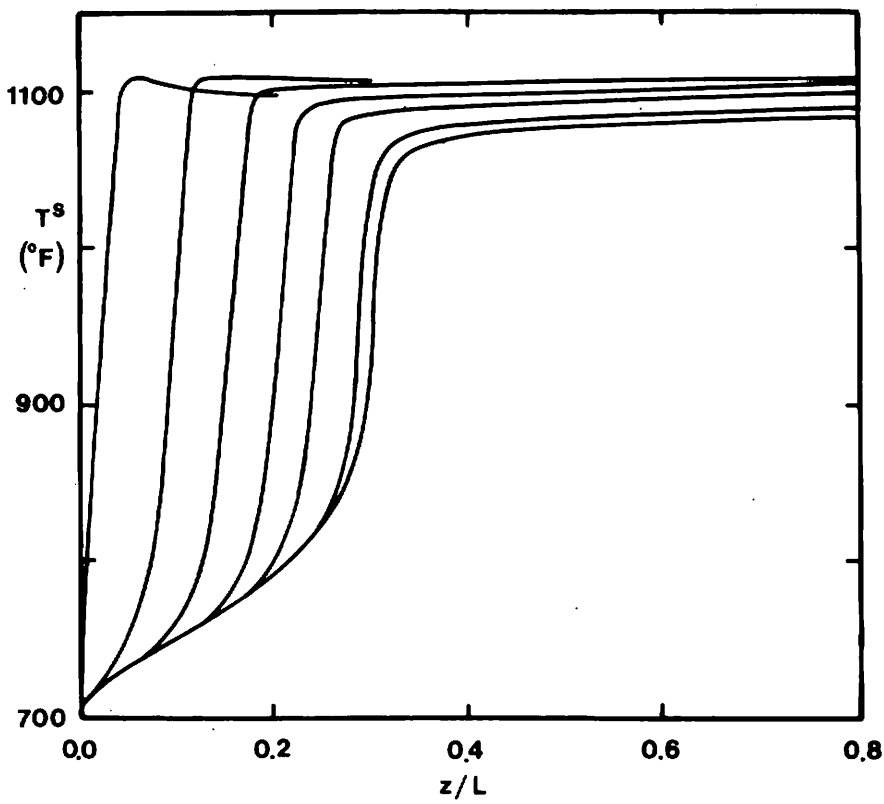

Fig. 5. Thermal Transient

variations of temperature and concentration are shown in Figure 7 for the cases given by curves 2 and 3 in Figure 6. Dispite large concentration variations around the periphery of the square, the profile in Figure 6 is shifted only shightly. This is why a single solid collocation point is used in the other duct shapes of Figure 2.

It is much more important that the fluid equations (3,4) be solved correctly. Figure 8 shows the errors incurred if only a single collocation point is used. Other calculations (Young and Finlayson, 1976) show even more dramatic differences.

5. Conclusion

The equations governing heat and mass transfer in monolith ducts can be modeled by a collocation method employing global orthogonal collocation, finite element orthogonal collocation, and an integro-differential technique. Steady-state calculations can be performed in about a second on an IBM 370/165 computer for situations involving 242 nonlinear algebraic equations. Without the integro-differential equation technique, the number of unknowns would have been increased to 1694, making the computations much more expensive. Transient simulations are only feasible with the integro-differential equation technique.

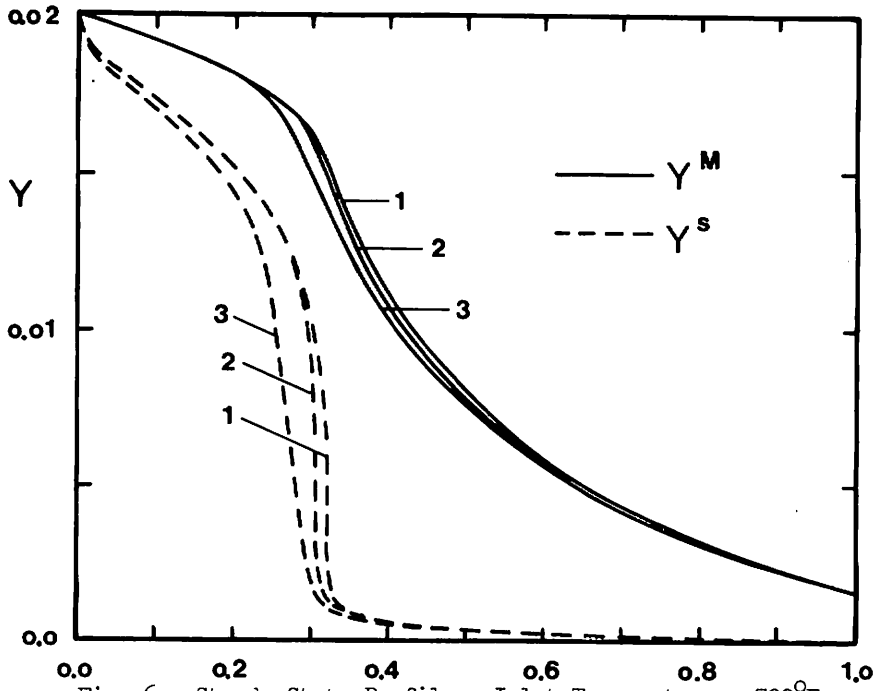

Fig. 6. Steady State Profiles, Inlet Temperature = 700°F

6. Acknowledgements

Acknowledgement is made to the donors of the Petroleum Research Fund, administered by the American Chemical Society, for support of this research under Grant PRF No. 7698-AC7. Thanks are also due to the Instituttet for Kemiteknik, Danmarks tekniske Højskole, 2800 Lyngby, Denmark, for providing computational, drafting, and secretarial facilities.

7. References

CAREY, G.F., and FINLAYSON, B.A. (1975): "Orthogonal Collocation on Finite Elements", Chem.Eng.Sci., Vol. 30. 587.

FINLAYSON, B.A. (1972): "The Method of Weighted Residuals and Variational Principles", Academic Press.

FINLAYSON, B.A. (1974): Ch. 1 in "Finite Elements in Fluids", Vol. 2, ed. Gallagher, R.H., Oden, J.T., Zienkiewicz, O.C., and Taylor, C., Wiley.

HARNED, J.L. (1972): "Analytical Evaluation of a Catalytic Converter System", Soc.Auto.Eng., paper 720520.

HLAVÁČEK, V. and VOTRUBA, J. (1974): "Experimental Study of Multiple Steady States in Adiabatic Catalytic Systems", Chem. Reaction Engng. - II, Adv.Chem.Ser., Vol. 133, 545.
(See also Erdöl and Kohle, Vol. 27, 261 (1974).

YOUNG, L.C. and FINLAYSON, B.A. (1976): "Mathematical Models of the Monolith Catalytic Converter. Parts I and II", Am.Inst. Chem.Eng. J., Vol. 22, (March issue).

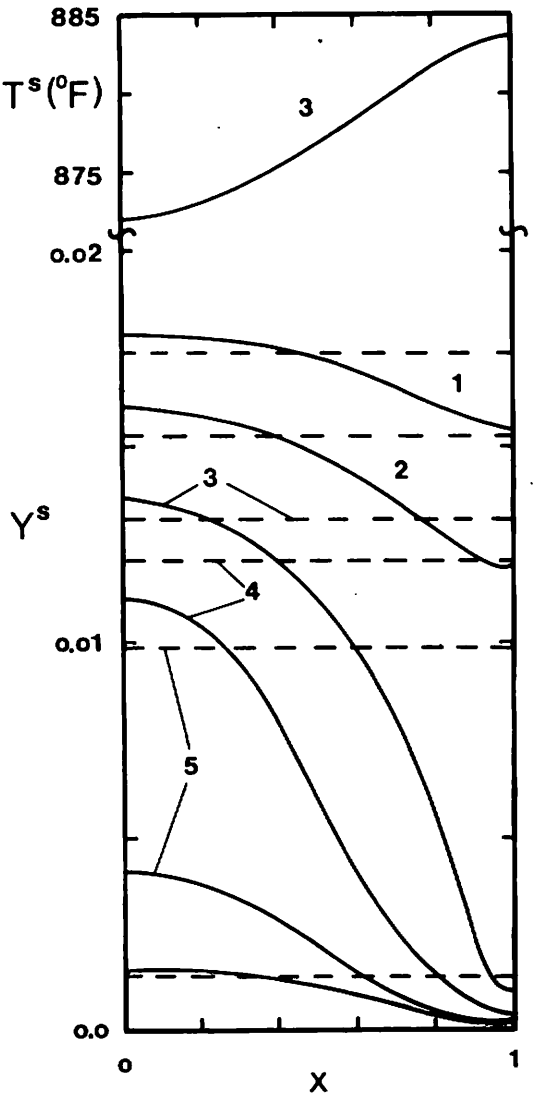

Fig. 7. Temperature and Mole Fraction in Walls of Solid. Same case as Figure 6

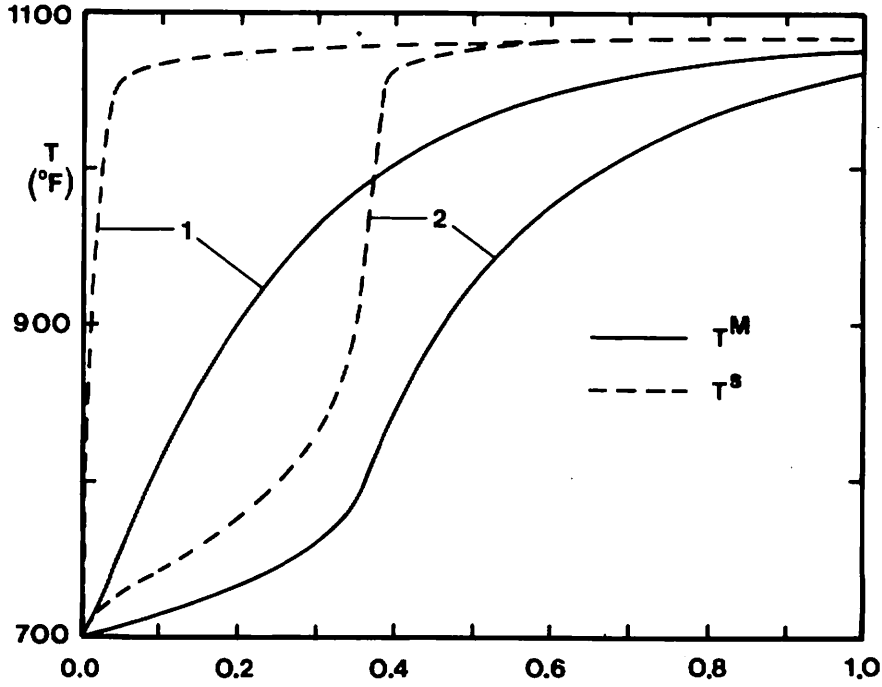

Fig. 8. Effect of Poor Approximation in the Fluid.
1-single collocation point, 2-three collocation points.